

The role of H₂SO₄-NH₃ anion clusters in ion-induced aerosol nucleation mechanisms in the boreal forest

Chao Yan¹, Lubna Dada¹, Clémence Rose¹, Tuija Jokinen¹, Wei Nie^{1,2}, Siegfried Schobesberger^{1,3}, Heikki Junninen^{1,4}, Katrianne Lehtipalo¹, Nina Sarnela¹, Ulla Makkonen⁵, Olga Garmash¹, Yonghong Wang¹, Qiaozhi Zha¹, Pauli Paasonen¹, Federico Bianchi¹, Mikko Sipilä¹, Mikael Ehn¹, Tuukka Petäjä^{1,2}, Veli-Matti Kerminen¹, Douglas R. Worsnop^{1,6}, Markku Kulmala^{1,2,7}

¹ Institute for Atmospheric and Earth System Research / Physics, Faculty of Science, University of Helsinki, P.O. Box 64, FI-00014, Helsinki, Finland

² Joint International Research Laboratory of Atmospheric and Earth System Sciences, School of Atmospheric Sciences, Nanjing University, Nanjing, 210046, P.R. China

³ Department of Applied Physics, University of Eastern Finland, 70211 Kuopio, Finland

⁴ Institute of Physics, University of Tartu, Ülikooli 18, EE-50090 Tartu, Estoni

⁵ Finnish Meteorological Institute, 00560 Helsinki, Finland.

⁶ Aerodyne Research, Inc., Billerica, MA 01821, USA

⁷ Aerosol and Haze Laboratory, Beijing Advanced Innovation Center for Soft Matter Science and Engineering, Beijing University of Chemical Technology, Beijing, 100029, P.R. China

Correspondence to: Chao Yan (chao.yan@helsinki.fi)

Abstract

New particle formation (NPF) provides a large source of atmospheric aerosols, which affect the climate and human health. Ion-induced nucleation (IIN) has been discovered as an important pathway of forming particles within recent chamber studies, however, atmospheric investigation remains incomplete. For this study, we investigated the air anion compositions in the boreal forest in Southern Finland for 3 consecutive springs, with a special focus on H₂SO₄-NH₃ anion clusters. We found that the ratio between the concentrations of highly oxygenated organic molecules (HOMs) and H₂SO₄ controlled the appearance of H₂SO₄-NH₃ clusters ($3 < \#S < 13$): All such clusters were observed when $[HOM]/[H_2SO_4]$ was smaller than 30. The number of H₂SO₄ molecules in the largest observable cluster correlated with the probability of ion-induced nucleation (IIN) occurrence, which reached almost 100 % when the largest observable cluster contained 6 or more H₂SO₄ molecules. During selected cases when the time evolution of H₂SO₄-NH₃ clusters could be tracked, the calculated ion growth rates exhibited a good agreement across measurement methods and cluster (particle) sizes. In these cases, H₂SO₄-NH₃ clusters alone could explain ion growth up to 3 nm (mobility diameter). IIN events also occurred in the absence of H₂SO₄-NH₃, implying that also other NPF mechanisms prevail at this site, most likely involving HOMs. It seems that H₂SO₄ and HOMs both affect the occurrence of an IIN event, but their ratio ($[HOMs]/[H_2SO_4]$) defines the primary mechanism

of the event. Since that ratio is strongly influenced by solar radiation and temperature, IIN mechanism ought to vary depending on conditions and seasons.

1 Introduction

Atmospheric aerosol particles are known to influence human health and the climate (Heal et al., 2012; Stocker et al., 2013). New particle formation (NPF) from gas-phase precursors contributes to a major fraction of the global cloud condensation nuclei population (Merikanto et al., 2009; Kerminen et al., 2012; Dunne et al., 2016; Gordon et al., 2017), and provides an important source of particulate air pollutants in many urban environments (Guo et al., 2014).

Although NPF is an abundant phenomenon and has been observed in different places around the globe within the boundary layer (Kulmala et al., 2004), the detailed mechanisms at each location may differ and are still largely unknown. Experiments done in the CLOUD chamber (Cosmic Leaving Outside Droplets) at CERN explored different NPF mechanisms on molecular level, including sulfuric acid (H_2SO_4) and ammonia (NH_3) nucleation (Kirkby et al., 2011), H_2SO_4 and dimethylamine (DMA) nucleation (Almeida et al., 2013), and pure biogenic nucleation (Kirkby et al., 2016) from highly oxygenated organic molecules (HOMs) (Ehn et al., 2014). While chamber experiments can mimic some properties of ambient observations (Schobesberger et al., 2013), it is still ambiguous to what extent these chamber findings can be applied to understand NPF in the more complex atmosphere, mostly due to the challenges in atmospheric measurements and characterization of the nucleating species.

In the aforementioned chamber studies, ions have been shown to play a crucial role in enhancing new particle formation, which is known as ion-induced nucleation (IIN). The importance of IIN varies significantly depending on the temperature as well as the concentration and composition of the ion species. For instance, big H_2SO_4 ion clusters were not found in the sulfur-rich airmass from Atlanta, suggesting the minor role of IIN (Eisele et al., 2006). Similar conclusions were drawn based on the observations in Boulder (Iida et al., 2006) and Hyytiälä (e.g., Manninen et al., 2010), although the suggested importance of IIN in cold environment, such as upper troposphere, cannot be excluded (Lovejoy et al., 2004; Kurten et al., 2016). Recent the CLOUD experiments have revealed that the importance of IIN can be negligible in the H_2SO_4 -DMA system (Almeida et al., 2013), moderate in the H_2SO_4 - NH_3 system (Kirkby et al., 2011) and dominating in the pure HOMs system (Kirkby et al., 2016). However, it is also important to note that the ion-pair concentration in Hyytiälä is lower than in the CLOUD chamber, which partly explains the its smaller contribution of IIN (Wagner et al., 2017).

The recently developed atmospheric-pressure-interface time-of-flight mass spectrometer (APi-TOF) (Junninen et al., 2010) has been used for measuring ion composition at the SMEAR II station in Hyytiälä since 2009. Ehn et al., (2010) have first shown that the negative ion population varied significantly, with H₂SO₄ clusters dominating during the day and HOM-NO₃⁻ clusters during the night. This variation was further studied by Bianchi et al., (2017), who grouped HOM-containing ions by separating the HOMs into non-nitrate- and nitrate-containing species as well as into ion adducts with HSO₄⁻ or NO₃⁻. In the night time, HOMs may form negatively charged clusters containing up to 40 carbons (Bianchi et al., 2017; Frege et al., 2018). In the daytime, H₂SO₄ and H₂SO₄-NH₃ clusters appear to be the most prominent negative ions (Schobesberger et al., 2015; Schobesberger et al., 2013). However, they have not yet been thoroughly studied regarding their appearance and their plausible links to atmospheric IIN.

Along with the changes in temperature and in ion concentration and composition, the importance of IIN is expected to vary considerably. In this study, we revisit the ion measurement in Hyytiälä, aiming to connect our current understanding of the formation of ion clusters to the significance of IIN, with a special focus on the fate of H₂SO₄-NH₃ clusters. We also extend our analysis to ions other than H₂SO₄ clusters, i.e., HOMs, and identify their role in IIN, in addition to other measured parameters on site. Finally, this study confirms the consistency between chamber findings and atmospheric observations, even though it seems that at least two separate mechanisms are alternatively controlling the IIN in Hyytiälä.

2 Materials and Methods

For this study, we used data collected at the Station for Measuring Forest Ecosystem-Atmospheric Relations (SMEAR II station), in Hyytiälä, Southern Finland (Hari and Kulmala, 2005). In this study, our data sets were obtained from intensive campaigns in 3 consecutive springs, 2011 – 2013. The exact time periods of the APi-TOF measurements are 22nd of March until 24th of May 2011, 31st March until 28th of April 2012, and 7th April until 8th of June 2013. For 134 days we were able to extend our analysis to include: i) ion composition and chemical characterization using the APi-TOF (Junninen et al., 2010), ii) particle and ion number size distribution using NAIS (e.g., Mirme and Mirme 2013), iii) concentrations of H₂SO₄ and HOMs measured by the chemical ionization atmospheric-pressure-interface time-of-flight mass spectrometer (CI-APi-TOF see, e.g., (Jokinen et al., 2012; Ehn et al., 2014; Yan et al.,

2016), and iv) other relevant parameters, e.g., NH_3 (Makkonen et al., 2014), temperature and cloudiness (Dada et al., 2017).

2.1 Measurement of atmospheric ions

The composition of atmospheric anions was measured using the atmospheric-pressure-interface time-of-flight mass spectrometer (APi-TOF) (Junninen et al., 2010). The instrument was situated inside a container in the forest, direct sampling the air outside. To minimize the sampling losses, we firstly drew the air at a larger flow rate within a wide tube (40 mm inner diameter), and another 30-cm-long coaxial tube (10 mm outer diameter and 8 mm inner diameter) inside the wider one was used to draw 5 L/min towards the APi-TOF, 0.8 L/min out of which will enter through the pinhole. After entering the pinhole, the ions are focused and guided through two quadrupoles and one ion lens, and finally and detected by the time-of-flight mass spectrometer.

Different from the commonly used chemical-ionization mass spectrometer (CIMS), the APi-TOF does not do any ionization, so it only measures the naturally charged ions in the sample. In the atmosphere, the ion composition is affected by the proton affinity of the species: Molecules with the lowest proton affinity are more likely to lose the proton and thus become negatively charged after colliding many times with other species; similarly, molecules with the highest proton affinity would probably become positively charged ions. In addition to the proton affinity, the neutral concentration also plays a role in determining the ion composition by affecting the collision frequency. Due to the limited ionization rate in the atmosphere, there is always a competition between different species in taking the charges. For example, the H_2SO_4 often dominates the spectrum in the daytime when it is abundant, while in the night-time nitrate ions and its cluster with HOMs are always the prominent due to the rare chance to collide with the H_2SO_4 . Since the signal strength of an ion in the APi-TOF depends not only on the abundance of the respective neutral molecules, but also on the availability of other charge-competing species, it is very important to note that the APi-TOF can not quantify the neutral species.

One important virtue of APi-TOF is that it does not introduce extra energy during sampling, which ensures the sample is least affected when compared to other measurement techniques such as CIMS. although fragmentation cannot be fully avoided inside the instrument (Schobesberger et al., 2013). Because of this, it is a well-suited instrument to directly measure the composition of weakly bonded clusters in the atmosphere.

The APi-TOF data were processed with the tofTools package (version 6.08) (Junninen et al., 2010). Since the ion signal in APi-TOF is usually weak, a 5-hour integration time was used, after which the signals of H₂SO₄-NH₃ clusters and HOMs were fitted (See Fig.1). For HOM signals, we used the same peaks reported in Bianchi et al., (2017), and the total signal of HOM ions is the sum of all identified HOMs.

It should also be mentioned that the voltage tuning of the instrument was not the same in the years we analyzed, which led to differences in the ion transmission efficiency function. For example, we noticed that in 2011, the largest H₂SO₄-NH₃ clusters contained 6 H₂SO₄ molecules, whereas more than 10 H₂SO₄ were observed in the clusters in other years. This was very likely due to the very low ion transmission in the mass range larger than about 700 Th for the measurements in 2011. However, this should not affect our results and conclusions, because clusters consisting of 6 H₂SO₄ molecules had little difference from larger clusters in affecting the IIN in terms of occurrence probability (see more details in Sect. 3.3.1).

2.2 Measurement of H₂SO₄ and HOMs

The concentrations of H₂SO₄ and HOMs were measured by the chemical ionization atmospheric-pressure-interface time-of-flight mass spectrometer (CI-APi-TOF). The details of the quantification method for H₂SO₄ can be found in Jokinen et al., (2012) and for HOMs in Kirkby et al., 2016. For all data, we applied the same calibration coefficient (1.89×10^{10} 1/cm³) reported by Jokinen et al., (2012).

Although the tuning of the CI-APi-TOF was not exactly the same during the measurement period included in this study, no systematic difference was found in the concentrations of H₂SO₄ and HOMs from different years.

2.3 Measurements of ion and particle size distribution

The mobility distribution of charged particles and air ions in the range 3.2-0.0013 cm²V⁻¹s⁻¹ (corresponding to mobility diameter 0.8 – 42 nm) were measured together with the size distribution of total particles in the range ~2.5 - 42 nm using a neutral cluster and air ion spectrometer (NAIS, Aired Ltd., (Mirme and Mirme, 2013)). The instrument has two identical differential mobility analyzers (DMA) which allow for the simultaneous monitoring of positive and negative ions. In order to minimize the diffusion losses in the sampling lines, each analyzer has a sample flow rate of 30 L min⁻¹ and a sheath flow rate of 60 L min⁻¹. In “particle mode”, when measuring total particle concentration, neutral particles are charged by ions produced from a corona discharge in a “pre-charging” unit before they are detected in the DMAs. The charging ions used in this process were previously reported to influence the total particle

concentrations below ~2 nm (Asmi et al., 2008; Manninen et al., 2010); for that reason, only the particle concentrations above 2.5 nm were used in the present work. Also, each measurement cycle, i.e. 2 min in ion mode and 2 min in particle mode, is followed by an offset measurement, during which the background signal of the instrument is determined and then subtracted from measured ion and particle concentrations. In addition, particle size distributions between 3 and 990 nm were measured with a differential mobility particle sizer (DMPS) described in details in Aalto et al., (2001). Based on earlier work by Kulmala et al., (2001), this data were used to calculate the condensation sink (CS), which represents the rate of loss of condensing vapors on pre-existing particles.

2.4 Measurement of Meteorological parameter

The meteorological variables used as supporting data in the present work were measured on a mast, all with a time resolution of 1 min. Temperature and relative humidity were measured at 16.8 m using a PT-100 sensor and relative humidity sensors (Rotronic Hygromet MP102H with Hygroclip HC2-S3, Rotronic AG, Bassersdorf, Switzerland), respectively. Global radiation was measured at 18 m with a pyranometer (Middleton Solar SK08, Middleton Solar, Yarraville, Australia), and further used to calculate the cloudiness parameter, as done previously by Dada et al., (2017, and references therein). This parameter is defined as the ratio of measured global radiation to theoretical global irradiance, so that parameter values < 0.3 correspond to a complete cloud coverage, while values > 0.7 are representative of clear sky conditions.

2.5 Calculation of particle formation rates and growth rates

The formation rate of 2.5 nm particles includes both neutral and charged particles, and it was calculated from the following equation:

$$J_{2.5} = \frac{dN_{2.5-3.5}}{dt} + CoagS_{2.5} \times N_{2.5-3.5} + \frac{1}{1nm} GR_{1.5-3} \times N_{2.5-3.5} \quad \text{Eq. 1}$$

where $N_{2.5-3.5}$ is the particle concentration between 2.5 and 3.5 nm measured with the NAIS in particle mode, $CoagS_{2.5}$ is the coagulation sink of 2.5 nm particles derived from DMPS measurements and $GR_{1.5-3}$ is the particle growth rate calculated from NAIS measurements in ion mode. Calculating the formation rate of 2.5 nm ions, or charged particles includes two additional terms to account for the loss of 2.5 – 3.5 nm ions due to their recombination with sub-3.5 nm ions of the opposite polarity (fourth term of Eq. 2) and the gain of ions caused by the attachment of sub-2.5 nm ions on 2.5-3.5 nm neutral clusters (fifth term of Eq. 2):

$$J_{2.5}^{\pm} = \frac{dN_{2.5-3.5}^{\pm}}{dt} + CoagS_{2.5} \times N_{2.5-3.5}^{\pm} + \frac{1}{1nm} GR_{1.5-3} \times N_{2.5-3.5}^{\pm} + \alpha \times N_{2.5-3.5}^{\pm} N_{<3.5}^{\mp} - \beta \times N_{2.5-3.5} N_{<2.5}^{\pm} \quad \text{Eq.2}$$

where $N_{2.5-3.5}^{\pm}$ is the concentration of positive or negative ions between 2.5 and 3.5 nm, $N_{<2.5}^{\pm}$ is the concentration of sub-2.5 nm ions of the same polarity and $N_{<3.5}^{\mp}$ is the concentration of sub-3.5 nm ions of the opposite polarity, all measured with the NAIS in ion mode. α and β are the ion-ion recombination and the ion-neutral attachment coefficients, respectively, and were assumed to be equal to $1.6 \times 10^{-6} \text{ cm}^3 \text{ s}^{-1}$ and $0.01 \times 10^{-6} \text{ cm}^3 \text{ s}^{-1}$, respectively. We consider these values as reasonable approximations, keeping in mind that the exact values of both α and β depend on a number of variables, including the ambient temperature, pressure and relative humidity as well as the sizes of the colliding objects (ion-ion or ion-aerosol particle) (e.g. Hoppel, 1985; Tammet and Kulmala, 2005; Franchin et al., 2015).

$GR_{1.5-3}$ were calculated from NAIS data in ion mode using the “maximum” method introduced by (Hirsikko et al., 2005). Briefly, the peaking time of the ion concentration in each size bin of the selected diameter range was first determined by fitting a Gaussian to the concentration. The growth rate was then determined by a linear least square fit through the times. The uncertainty in the peak time determination was reported as the Gaussian’s mean 67% confidence interval, and was further taken into account in the growth rate determination.

A similar approach was used to estimate the early growth rate of the $\text{H}_2\text{SO}_4\text{-NH}_3$ clusters detected with the APi-TOF. Prior to growth rate calculation, we first converted cluster masses into diameters in order to get growth rate values in nm h^{-1} instead of amu h^{-1} . For that purpose, we applied the conversion from Ehn et al., (2011), using a cluster density of 1840 kg m^{-3} . The time series of the cluster signals were then analysed in the same way as ion or particle concentrations using the “maximum” method from Hirsikko et al. (2005), and the growth rate was calculated using the procedure recalled above. Our ability to determine the early cluster growth rate from APi-TOF measurement was strongly dependent on the strength of the signal of the different $\text{H}_2\text{SO}_4\text{-NH}_3$ clusters. As a consequence, the reported growth rates characterize a size range which might slightly vary between the events, falling in a range between 1 and 1.7 nm.

3 Results and Discussion

3.1 Daytime ion composition

We examined the daytime ion composition of 134 days from three consecutive springs (2011-2013) in Hyytiälä. Consistent with the findings by previous studies, showing that H_2SO_4

clusters are the most abundant ions in the daytime (Ehn et al., 2010; Bianchi et al., 2017), we found that NH_3 -free H_2SO_4 clusters can contain up to three H_2SO_4 molecules when counting the HSO_4^- also as one H_2SO_4 molecule ($(\text{H}_2\text{SO}_4)_2\text{HSO}_4^-$), and that NH_3 is always present in clusters containing 4 or more H_2SO_4 molecules. The latter feature suggests the important role of NH_3 as a stabilizer in growing H_2SO_4 clusters (Kirkby et al. 2011). NH_3 -free clusters (at least dimers $\text{H}_2\text{SO}_4\text{HSO}_4^-$) were observed on 116 measurement days, but the signal intensity varied from day to day. Bigger clusters that contained NH_3 were observed on 39 days, containing a maximum of 4 to 13 H_2SO_4 per cluster. Figure 1 provides four examples of daytime ion spectra, including an NH_3 -free case (Fig. 1A) and three cases with a different maximum size of $\text{H}_2\text{SO}_4\text{-NH}_3$ clusters (Fig. 1B-D), illustrating the significant variations in signal and maximum size of $\text{H}_2\text{SO}_4\text{-NH}_3$ clusters. In the NH_3 -free case, a larger number of HOM clusters (green circles) was observed, indicating a competition between H_2SO_4 and HOMs in taking the charges. The largest detected cluster during the measurement was $(\text{H}_2\text{SO}_4)_{12}(\text{NH}_3)_{13}\text{HSO}_4^-$, which corresponds to a mobility-equivalent diameter of about 1.7 nm according to the conversion method (Ehn et al., 2011) and is big enough to be detected by particle counters. Since the observed formation of such large $\text{H}_2\text{SO}_4\text{-NH}_3$ clusters is essentially the initial step of IIN, we anticipate that the variation of $\text{H}_2\text{SO}_4\text{-NH}_3$ clusters will influence the occurrence of IIN.

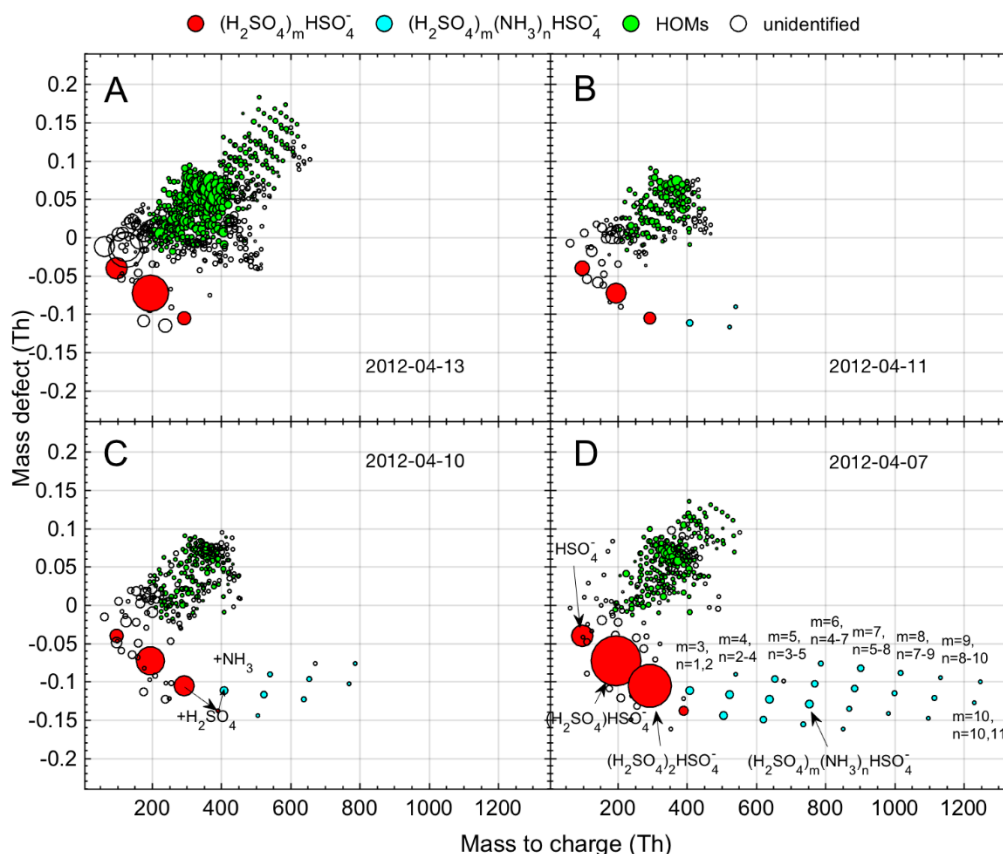


Figure 1 Mass defect plot showing the composition of ion clusters on four separate days. A) NH_3 -free clusters, B,C,D) H_2SO_4 - NH_3 clusters with different maximum number of H_2SO_4 molecules. The circle size is linearly proportional to the logarithm of the signal intensity.

3.2 The determining parameters for H_2SO_4 - NH_3 cluster formation

To find out the dominating parameters that affect the formation of H_2SO_4 - NH_3 clusters, we performed a correlation analysis that included the ambient temperature, relative humidity (RH), wind speed, wind direction, condensation sink (CS), as well as the gas-phase concentrations of NH_3 , H_2SO_4 , and HOMs. Among all the examined parameters, we found that the ratio between concentrations of HOMs and H_2SO_4 had the most pronounced influence on the appearance of H_2SO_4 - NH_3 clusters. As shown in Figure 2, all H_2SO_4 - NH_3 clusters were detected when $[\text{HOMs}]/[\text{H}_2\text{SO}_4]$ was smaller than 30. No such dependence was observed for only $[\text{HOMs}]$ or $[\text{H}_2\text{SO}_4]$. This implies that the appearance of H_2SO_4 - NH_3 clusters is primarily controlled by the competition between H_2SO_4 and HOMs in getting the charges. More specifically, HSO_4^- , the main charge carrier in the daytime, may either collide with neutral H_2SO_4 to form large clusters to accommodate NH_3 , or collide with HOMs that prevents the former process. In addition, a reasonable correlation was found between $[\text{HOMs}]/[\text{H}_2\text{SO}_4]$ and temperature, likely

explained by emission of volatile organic compounds (VOC) increasing with temperature, leading to higher HOMs concentrations, whereas the formation of H_2SO_4 is not strongly temperature-dependent. This observation indicates that the formation of $\text{H}_2\text{SO}_4\text{-NH}_3$ clusters may vary seasonally: we expect to see them more often in cold seasons when HOM concentrations are low, and less often in warm seasons.

Parameters other than $[\text{HOMs}]/[\text{H}_2\text{SO}_4]$ and temperature seemed to have little influence on the formation of $\text{H}_2\text{SO}_4\text{-NH}_3$ clusters. Interestingly, we found that NH_3 was even lower when $\text{H}_2\text{SO}_4\text{-NH}_3$ clusters were observed, indicating that the NH_3 concentration is not the limiting factor for forming $\text{H}_2\text{SO}_4\text{-NH}_3$ clusters (also see section 3.4). In addition, $\text{H}_2\text{SO}_4\text{-NH}_3$ clusters were observed in a wide range of RH spanning from 20 to 90 %, suggesting that RH is not affecting the cluster formation. Besides, no clear influence from condensation sink (CS), wind speed, or wind direction was observed.

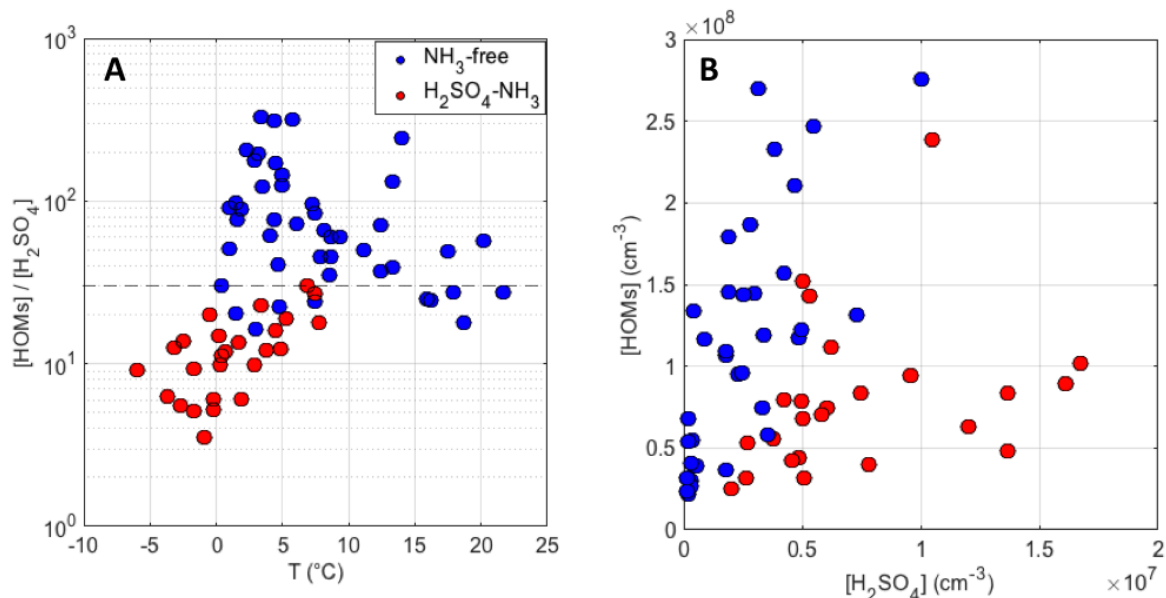


Figure 2 The effect of concentration of HOMs, H_2SO_4 , their ratio ($[\text{HOM}]/[\text{H}_2\text{SO}_4]$), and temperature on the appearance of $\text{H}_2\text{SO}_4\text{-NH}_3$ clusters.

3.3 The relation between $\text{H}_2\text{SO}_4\text{-NH}_3$ clusters and IIN

3.3.1 The effect of cluster size on the probability of IIN events

We identified IIN events using data from the NAIS (ion mode) by observing an increase in the concentration of sub-2 nm ions (Rose et al., 2018), and classified 67 IIN events out of the 134 days of measurements. We defined the IIN probability as the number of days when IIN events were identified out of the total number of days that were counted. For example, the overall IIN probability is 50 % (67 out of 134 days). We found that the maximum observed size of $\text{H}_2\text{SO}_4\text{-}$

NH₃ clusters may affect the occurrence of IIN. Our conclusion is complementary to previous theories which stated that the critical step of particle nucleation is the formation of initial clusters that are big enough for condensational growth to outcompete evaporation (Kulmala et al., 2013). To further understand the size-dependency of IIN probability, we investigated the IIN probability when different maximum sizes of H₂SO₄-NH₃ clusters were observed. As illustrated in Figure 3, the IIN probability increases dramatically when larger H₂SO₄-NH₃ clusters were observed: IIN events were never observed when only HSO₄⁻ or H₂SO₄HSO₄⁻ were present, whereas the IIN probability increased to about 50 – 60 % when the largest clusters contained 3 – 5 H₂SO₄ molecules. IIN occurred in 24 out of 25 days (96 %) when the largest clusters consisted of no less than 6 H₂SO₄ molecules. Thus, it is evident that the occurrence of IIN is related to the size and thus the stability of H₂SO₄-NH₃ clusters, and that a cluster consisting of 6 H₂SO₄ molecules seems to lie on the threshold size of triggering nucleation.

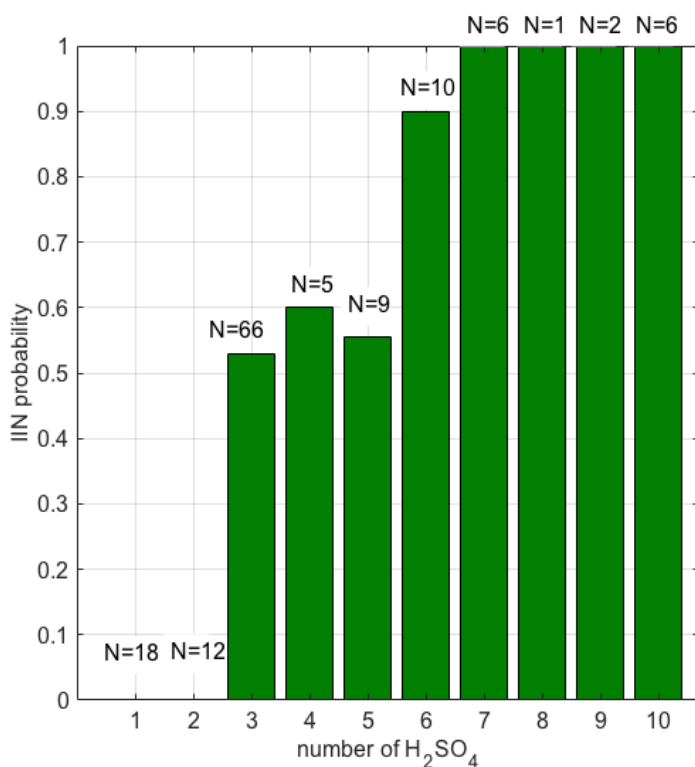


Figure 3 The maximum number of H₂SO₄ molecules observed in clusters and the respective IIN probability. The days when it was unclear if IIN occurred was counted as non-event days. N denotes the number of days when such clusters were the largest observed.

3.3.2 Continuous growth from clusters to 3 nm particles

Although the strong connection between the size of H₂SO₄-NH₃ clusters and the occurrence of IIN was confirmed, it is challenging to directly observe the growth of these clusters in the

atmosphere, limited by the inhomogeneity of the ambient air and low concentrations of atmospheric ions. Combining APi-TOF and NAIS measurements, we were able to follow the very first steps of the cluster growth for 8 of the detected events. In Figures 4A and 4B, we present two examples in which the continuous growth of $\text{H}_2\text{SO}_4\text{-NH}_3$ clusters to 3 nm (mobility diameter) particles was directly evaluated using the maximum-time method. The maximum times, determined from APi-TOF and NAIS data independently, fall nicely on the same linear fit. The continuity of the growth and the linearity of the fit suggests that the current mechanism ($\text{H}_2\text{SO}_4\text{-NH}_3$, acid-base) explains the formation and growth of sub-3 nm ion clusters in these cases. In most cases, the calculation of cluster GR from APi-TOF measurement suffered from high uncertainties, but a weak positive correlation can be observed between the cluster growth rate and H_2SO_4 concentration (Fig. 4C). This correlation is likely due to the collision of H_2SO_4 with existing $\text{H}_2\text{SO}_4\text{-NH}_3$ clusters being the limiting step for cluster growth when NH_3 is abundant enough to follow up immediately (Schobesberger et al., 2015).

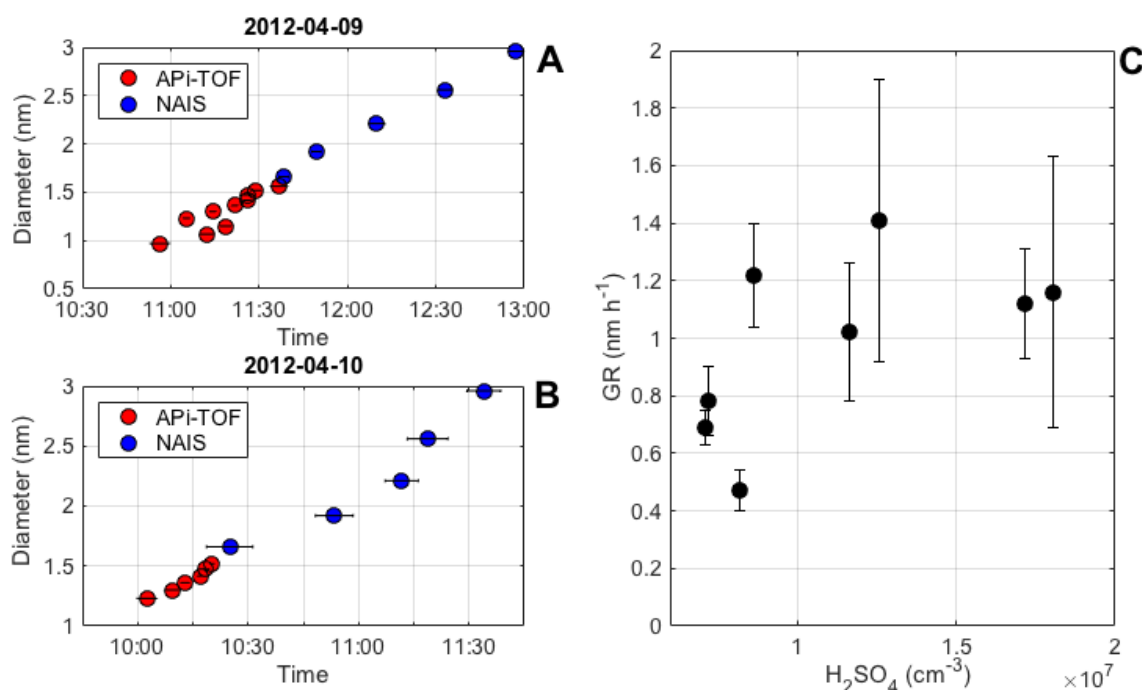


Figure 4 Cluster growth rate determined from APi-TOF (A) and NAIS (B) measurements using the maximum time method, and the correlation between growth rates and concentrations of H_2SO_4 molecules (C).

3.4 Evidence for other IIN mechanisms

328 For the 134 days of measurements, we were able to identify 67 IIN events using the NAIS data,
 329 out of which $\text{H}_2\text{SO}_4\text{-NH}_3$ clusters were observed on 32 days, implying that at least 35 IIN
 330 events were likely driven by mechanism(s) other than $\text{H}_2\text{SO}_4\text{-NH}_3$. In Figure 5, we classified
 331 the days according to the types of IIN observation: 32 IIN events involving $\text{H}_2\text{SO}_4\text{-NH}_3$ (S-E),
 332 3 non-events with the presence of $\text{H}_2\text{SO}_4\text{-NH}_3$ clusters (S-NE), 35 IIN events involving other
 333 mechanisms (O-E), 41 other non-event days (O-NE), and 23 days with unclear types. We
 334 further present the respective statistics of additional measurements for the first four types of
 335 days, including the concentrations of plausible precursor vapors, condensation sink and
 336 meteorological parameters. It should be noted that the SA-NE has only 3 days, thus the statistics
 337 on this type of days might not be fully representative.

338 Consistent with the previous discussion (Fig. 2), low temperatures are conducive of IIN events
 339 via the $\text{H}_2\text{SO}_4\text{-NH}_3$ mechanism whilst being the highest other type of events (O-E) (Fig. 5A).
 340 The clear-sky parameter (100% = clear sky and 0% = cloudiness) shows a noticeably higher
 341 value during both event types compared to the non-event cases (Fig. 5B), indicating that photo-
 342 chemistry related processes are important for all events. Moreover, the CS is obviously lower
 343 for both types of events than on non-event days (Fig. 5C). Although a strong effect of CS on
 344 the appearance of $\text{H}_2\text{SO}_4\text{-NH}_3$ clusters has not been noticed, it is a most important parameter
 345 in regulating the occurrence of IIN. Similar effects of cloudiness and CS on governing the
 346 occurrence of NPF have been reported by Dada et al., (2017) based on long-term data sets.

347 Remarkably, NH_3 has very low concentrations during $\text{H}_2\text{SO}_4\text{-NH}_3$ events in comparison to the
 348 other type of events (Fig. 5D). This is likely due to high NH_3 concentrations coinciding with
 349 higher temperature and thus elevated HOMs concentration, or the lower stability of $\text{H}_2\text{SO}_4\text{-}$
 350 NH_3 clusters at high temperatures that can evaporate NH_3 back to the atmosphere. This
 351 observation rules out the addition of NH_3 as a limiting step in the $\text{H}_2\text{SO}_4\text{-NH}_3$ nucleation
 352 mechanism, but the participation of NH_3 in the other type of events cannot be excluded.

353 H_2SO_4 has the highest concentrations during the $\text{H}_2\text{SO}_4\text{-NH}_3$ -involved events (Fig. 5E), but the
 354 concentration of H_2SO_4 in S-NE days is not much lower, suggesting that the occurrence of
 355 $\text{H}_2\text{SO}_4\text{-NH}_3$ -involved events is not solely controlled by the H_2SO_4 concentration. The
 356 Incorporating the effect of CS ($[\text{H}_2\text{SO}_4]/\text{CS}$) significantly improves the separation (Fig. 5F).
 357 McMurry and coworkers (McMurry et al., 2005) have introduced a parameter L (Eq.3) to
 358 quantitatively evaluate the likelihood of NPF, and they found that NPF mostly occurred when
 359 L is smaller than 1. A similar result has been reported by Kuang et al., (2010), and a slightly
 360 different threshold L value of 0.7 was determined.

$$L = \frac{CS}{[H_2SO_4]} \cdot \frac{1}{\beta_{11}} \text{ (Eq.3)}$$

Here, L is dimensionless parameter representing the probability that NPF will not occur, and β_{11} is the collision rate between H_2SO_4 vapor molecules, which is characterized as $4.4 \times 10^{-10} \text{ cm}^3 \text{ s}^{-1}$. Our results suggest a consistent L that most (75 percentile) S-E cases happen when L is lower than 0.73 and most (75 percentile) S-NE cases are observed when L is larger than 1.54. HOM concentrations are highest in the case of other events, revealing that HOMs play a key role in this mechanism (Fig. 5F), although the contribution of H_2SO_4 in this HOM-involving IIN mechanism cannot be excluded. Similar to the H_2SO_4 - NH_3 -driven cases, incorporating the CS better distinguishes the event and non-event cases. Overall, our results suggest that the concentrations of H_2SO_4 and HOMs, together with the CS governs the occurrence of IIN, whereas their ratio determines the exact underlying mechanism (Fig. 2). Although H_2SO_4 - NH_3 and HOMs clearly drives the S-E and O-E events, respectively, we cannot exclude the later participation of HOMs in SA-E cases or H_2SO_4 in O-E cases. Different NPF mechanisms have also been identified at the Jungfraujoch station (Bianchi et al., 2016) Frege et al., 2018) when influenced by different air masses. At SMEAR II station, on the other hand, our results suggest that the natural variation of temperature is already sufficient to modify the NPF mechanism via modulating the biogenic VOC emissions.

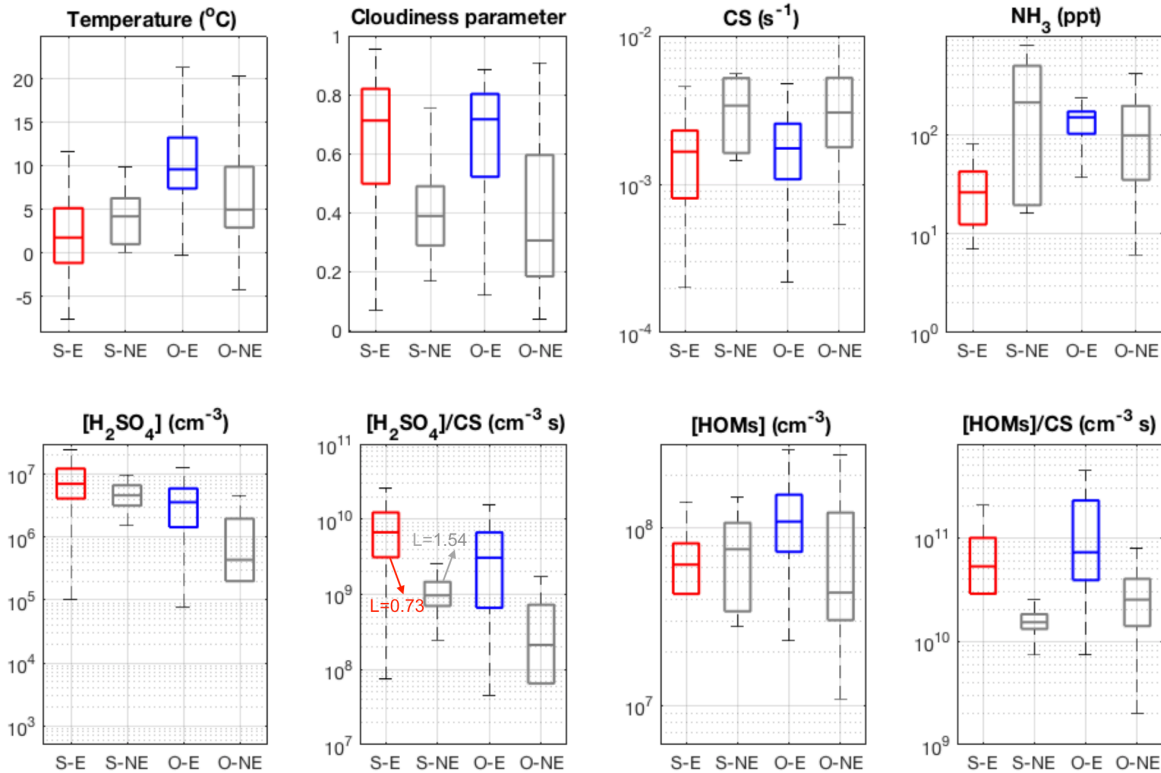


Figure 5 Comparison of different parameters for H₂SO₄-NH₃-involved events (S-E, red bars), non-events with the presence of H₂SO₄-NH₃ clusters (S-NE, first column of black bars), other events (O-E, blue bars), and other non-events (O-NE, second column of black bars).

3.5 Contribution of IIN to total nucleation rate

In order to get further insight into the importance of IIN during our measurements, we compared the formation rate of 2.5 nm ions, $J_{\text{ION}} = J_{2.5^{\pm}}$ (see Eq.2), to the total formation rate of 2.5 nm particles, $J_{\text{TOT}} = J_{2.5}$ (see Eq.1). The ratio $J_{\text{ION}}/J_{\text{TOT}}$ is equal to the charged fraction of the 2.5 nm particle formation rate. In analyzing field measurements, a similar ratio at a certain particle size (typically 2 nm) has commonly been used to estimate the contribution of ion-induced nucleation to the total nucleation rate (see Hirsikko et al. 2011 and references therein). It should be noted that $J_{\text{ION}}/J_{\text{TOT}}$ represents only a lower limit for the contribution of ion-induced nucleation, as this ratio does not take into account the potential neutralization of growing charged sub-2.5 nm particles by ion-ion recombination (e.g. Kontkanen et al., 2013; Wagner et al., 2017). At present, measuring the true contribution of ion-induced nucleation to the total nucleation rate is possible only in the CLOUD chamber (Wagner et al., 2017).

We were able to calculate J_{ION} and J_{TOT} for 57 (out of 67) cases, and the ratio $J_{\text{ION}}/J_{\text{TOT}}$ varied from 4 to 45%, showing a clear correlation with the HOM signal (Fig. 6A). This indicates the participation of HOMs even in H₂SO₄-NH₃-driven cases. In addition, most of the high $J_{\text{ION}}/J_{\text{TOT}}$ ratios were observed at moderate or low H₂SO₄ concentrations, e.g., $J_{\text{ION}}/J_{\text{TOT}} > 15\%$ was only observed when $[\text{H}_2\text{SO}_4] < 6 \times 10^6 \text{ cm}^{-3}$. These observations indicate that HOMs are important in high $J_{\text{ION}}/J_{\text{TOT}}$ cases, while during events driven by H₂SO₄-NH₃ clusters low $J_{\text{ION}}/J_{\text{TOT}}$ is more often observed. Accordingly, the median value of $J_{\text{ION}}/J_{\text{TOT}}$ for the H₂SO₄-NH₃ cases is about 12 % and is clearly higher (18 %) in HOM-driven events (Fig. 6D). Figures 6B and 6C reveal that both J_{ION} and J_{TOT} values are in fact higher in H₂SO₄-NH₃ cases, but the neutral nucleation pathway is relatively more enhanced, leading to the lower ratio. These results suggest that ion-induced nucleation plays a more important role in the events driven by HOMs than in the events driven by H₂SO₄-NH₃. A plausible explanation is that NH₃ is performing well in stabilizing H₂SO₄ molecules during the clustering process, whereas ions are a relatively more important stabilizing agent for HOM clustering.

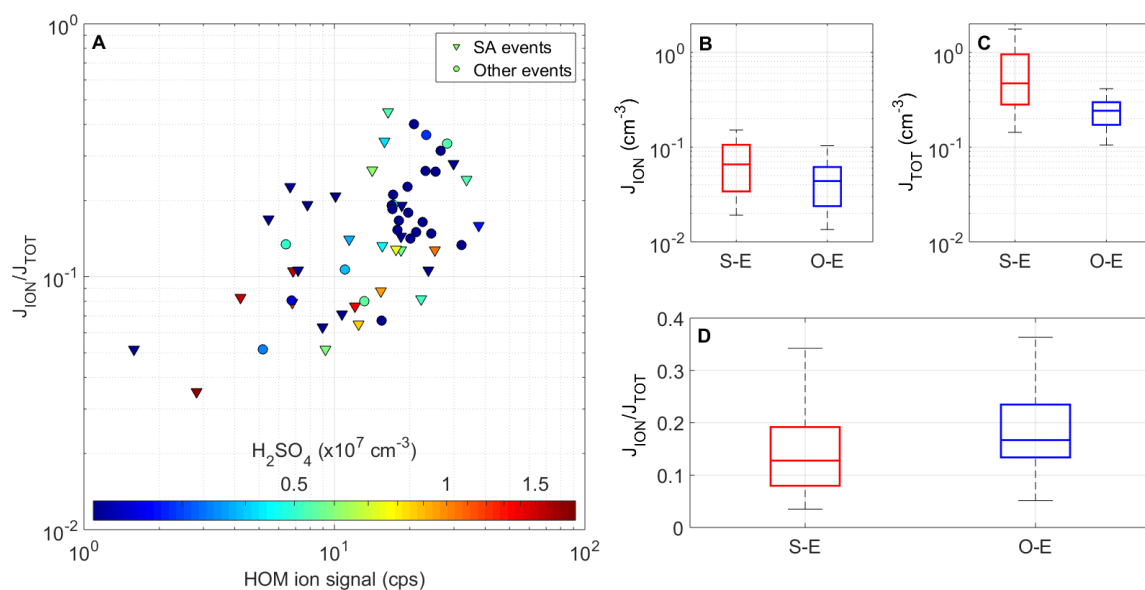


Figure 6. Formation rate 2.5 nm ions and total particles (both ions and neutral clusters) under different nucleation mechanisms. A) Charged fraction of the formation rate of 2.5 nm particles as a function of the total signal of HOM ions color-coded by the H_2SO_4 concentration, and (B, C and D) the differences in J_{ION} , J_{TOT} , and $J_{\text{ION}}/J_{\text{TOT}}$ between the H_2SO_4 - NH_3 -involved events (S-E) and other events (O-E).

4 Summary

We investigated the formation of H_2SO_4 - NH_3 anion clusters measured by APi-TOF during three springs from 2011 to 2013 in a boreal forest in Southern Finland and their connection to IIN. The abundance and maximum size of H_2SO_4 - NH_3 clusters showed great variability. Out of the total 134 measurement days, H_2SO_4 - NH_3 clusters were only seen during 39 days. The appearance of these clusters was mainly regulated by the concentration ratio between HOMs and H_2SO_4 , which can be changed by temperature via modulating the HOM production.

We found that the maximum observable size of H_2SO_4 - NH_3 clusters has a strong influence on the probability of an IIN event to occur. More specifically, when clusters containing 6 or more H_2SO_4 molecules were detected, IIN was observed at almost 100% probability. We further compared the cluster ion growth rates from APi-TOF and NAIS using the maximum-time method. In these H_2SO_4 - NH_3 driven cases when we could robustly define the track of the cluster evolution, the cluster growth was continuous and near linear for cluster-sizes up to 3 nm, suggesting co-condensation of H_2SO_4 and NH_3 as the sole growth mechanism. This does not exclude that organics could also participate in the growth process in Hyytiälä on other days. In addition, we noticed that there was a mechanism driving the IIN, and HOMs are the most likely responsible species, although H_2SO_4 and NH_3 might also participate in this mechanism.

Such mechanism was responsible for at least 35 IIN events during the measurement days and is expected to be the prevailing one in higher-temperature seasons.

The contribution of IIN to the total rates of NPF differs between events driven by H₂SO₄-NH₃ and by HOMs. IIN plays a bigger role in HOM-driven events, likely due to a relatively stronger stabilizing effect of ions. Since the production of HOMs and H₂SO₄ are strongly modulated by solar radiation and/or temperature, a seasonal variation of IIN can be expected, not only in terms of frequency, but also in terms of the underlying mechanisms, and hence in terms of the enhancing effect of ions. This information should be considered in aerosol formation modelling in future works.

Acknowledgement

This work was partially funded by Academy of Finland (1251427, 1139656, 296628, 306853, Finnish centre of excellence 1141135), the EC Seventh Framework Program and European Union's Horizon 2020 program (Marie Curie ITN no. 316662 "CLOUD-TRAIN", no. 656994 "Nano-CAVa", no. 227463 "ATMNUCLE", no. 638703 "COALA", no. 714621 "GASPARCON", and no.742206 "ATM-GTP"), European Regional Development Fund project "MOBTT42". We thank the tofTools team for providing tools for mass spectrometry analysis.

References

- Aalto, P., Hämeri, K., Becker, E., Weber, R., Salm, J., Mäkelä, J. M., Hoell, C., O'Dowd, C. D., Karlsson, H., and Hansson, H. C.: Physical characterization of aerosol particles during nucleation events, *Tellus B*, 53, 344–358, 2001.
- Almeida, J., Schobesberger, S., Kuerten, A., Ortega, I. K., Kupiainen-Maatta, O., Praplan, A. P., Adamov, A., Amorim, A., Bianchi, F., Breitenlechner, M., David, A., Dommen, J., Donahue, N. M., Downard, A., Dunne, E., Duplissy, J., Ehrhart, S., Flagan, R. C., Franchin, A., Guida, R., Hakala, J., Hansel, A., Heinritzi, M., Henschel, H., Jokinen, T., Junninen, H., Kajos, M., Kangasluoma, J., Keskinen, H., Kupc, A., Kurten, T., Kvashin, A. N., Laaksonen, A., Lehtipalo, K., Leiminger, M., Leppä, J., Loukonen, V., Makhmutov, V., Mathot, S., McGrath, M. J., Nieminen, T., Olenius, T., Onnela, A., Petaja, T., Riccobono, F., Riipinen, I., Rissanen, M., Rondo, L., Ruuskanen, T., Santos, F. D., Sarnela, N., Schallhart, S., Schnitzhofer, R., Seinfeld, J. H., Simon, M., Sipila, M., Stozhkov, Y., Stratmann, F., Tome, A., Troestl, J., Tsagkogeorgas, G., Vaattovaara, P., Viisanen, Y., Virtanen, A., Vrtala, A., Wagner, P. E., Weingartner, E., Wex, H., Williamson, C., Wimmer, D., Ye, P., Yli-Juuti, T., Carslaw, K. S., Kulmala, M., Curtius, J., Baltensperger, U., Worsnop, D. R., Vehkamäki, H., and Kirkby, J.: Molecular understanding of sulphuric acid-amine particle nucleation in the atmosphere, *Nature*, 502, 359–363, 10.1038/nature12663, 2013.

469 Asmi, E., Sipilä, M., Manninen, H. E., Vanhanen, J., Lehtipalo, K., Gagne, S., Neitola, K.,
 470 Mirme, A., Mirme, S., Tamm, E., Uin, J., Komsaare, K., Attoui, M., and Kulmala, M.: Results
 471 of the first air ion spectrometer calibration and intercomparison workshop, *Atmospheric*
 472 *Chemistry and Physics*, 9, 141-154, 2009.

473 Bianchi, F., Tröstl, J., Junninen, H., Frege, C., Henne, S., Hoyle, C. R., Molteni, U., Herrmann,
 474 E., Adamov, A., Bukowiecki, N., Chen, X., Duplissy, J., Gysel, M., Hutterli, M., Kangasluoma,
 475 J., Kontkanen, J., Kürten, A., Manninen, H. E., Münch, S., Peräkylä, O., Petäjä, T., Rondo, L.,
 476 Williamson, C., Weingartner, E., Curtius, J., Worsnop, D. R., Kulmala, M., Dommen, J., and
 477 Baltensperger, U.: New particle formation in the free troposphere: A question of chemistry and
 478 timing, *Science*, doi:10.1126/science.aad5456, 2016.

479 Bianchi, F., Garmash, O., He, X., Yan, C., Iyer, S., Rosendahl, I., Xu, Z., Rissanen, M. P.,
 480 Riva, M., Taipale, R., Sarnela, N., Petaja, T., Worsnop, D. R., Kulmala, M., and Junninen, H.:
 481 The role of highly oxygenated molecules (HOMs) in determining the composition of ambient
 482 ions in the boreal forest, *Atmospheric Chemistry and Physics*, 17, 13819-13831, 2017.
 483

484 Dada, L., Paasonen, P., Nieminen, T., Mazon, S. B., Kontkanen, J., Perakyla, O., Lehtipalo,
 485 K., Hussein, T., Petaja, T., Kerminen, V. M., Back, J., and Kulmala, M.: Long-term analysis
 486 of clear-sky new particle formation events and nonevents in Hyytiälä, *Atmospheric Chemistry*
 487 *and Physics*, 17, 6227-6241, 10.5194/acp-17-6227-2017, 2017.
 488

489 Eisele, F., Lovejoy, E., Kosciuch, E., Moore, K., Mauldin, R., Smith, J., McMurry, P., and Iida,
 490 K.: Negative atmospheric ions and their potential role in ion-induced nucleation, *Journal of*
 491 *Geophysical Research: Atmospheres*, 111, 2006.
 492

493 Ehn, M., Junninen, H., Petaja, T., Kurten, T., Kerminen, V. M., Schobesberger, S., Manninen,
 494 H. E., Ortega, I. K., Vehkamäki, H., Kulmala, M., and Worsnop, D. R.: Composition and
 495 temporal behavior of ambient ions in the boreal forest, *Atmospheric Chemistry and Physics*,
 496 10, 8513-8530, 10.5194/acp-10-8513-2010, 2010.
 497

498 Ehn, M., Junninen, H., Schobesberger, S., Manninen, H. E., Franchin, A., Sipilä, M., Petaja,
 499 T., Kerminen, V. M., Tammet, H., Mirme, A., Mirme, S., Horrak, U., Kulmala, M., and
 500 Worsnop, D. R.: An Instrumental Comparison of Mobility and Mass Measurements of
 501 Atmospheric Small Ions, *Aerosol Science and Technology*, 45, 522-532,
 502 10.1080/02786826.2010.547890, 2011.
 503

504 Ehn, M., Kleist, E., Junninen, H., Petaja, T., Lonn, G., Schobesberger, S., Dal Maso, M.,
 505 Trimborn, A., Kulmala, M., Worsnop, D. R., Wahner, A., Wildt, J., and Mentel, T. F.: Gas
 506 phase formation of extremely oxidized pinene reaction products in chamber and ambient air,
 507 *Atmospheric Chemistry and Physics*, 12, 5113-5127, 10.5194/acp-12-5113-2012, 2012.
 508

509 Ehn, M., Thornton, J. A., Kleist, E., Sipilä, M., Junninen, H., Pullinen, I., Springer, M., Rubach,
 510 F., Tillmann, R., Lee, B., Lopez-Hilfiker, F., Andres, S. Y., Acir, I. H., Rissanen, M., Jokinen,
 511 T., Schobesberger, S., Kangasluoma, J., Kontkanen, J., Nieminen, T., Kurten, T., Nielsen, L.
 512 B., Jorgensen, S., Kjaergaard, H. G., Canagaratna, M., Dal Maso, M., Berndt, T., Petaja, T.,
 513 Wahner, A., Kerminen, V. M., Kulmala, M., Worsnop, D. R., Wildt, J., and Mentel, T. F.: A
 514 large source of low-volatility secondary organic aerosol, *Nature*, 506, 476-480,
 515 10.1038/nature13032, 2014.
 516

- Frege, C., Ortega, I. K., Rissanen, M. P., Praplan, A. P., Steiner, G., Heinritzi, M., Ahonen, L., Amorim, A., Bernhammer, A. K., Bianchi, F., Brilke, S., Breitenlechner, M., Dada, L., Dias, A., Duplissy, J., Ehrhart, S., El-Haddad, I., Fischer, L., Fuchs, C., Garmash, O., Gonin, M., Hansel, A., Hoyle, C. R., Jokinen, T., Junninen, H., Kirkby, J., Kurten, A., Lehtipalo, K., Leiminger, M., Mauldin, R. L., Molteni, U., Nichman, L., Petaja, T., Sarnela, N., Schobesberger, S., Simon, M., Sipila, M., Stolzenburg, D., Tome, A., Vogel, A. L., Wagner, A. C., Wagner, R., Xiao, M., Yan, C., Ye, P. L., Curtius, J., Donahue, N. M., Flagan, R. C., Kulmala, M., Worsnop, D. R., Winkler, P. M., Dommen, J., and Baltensperger, U.: Influence of temperature on the molecular composition of ions and charged clusters during pure biogenic nucleation, *Atmospheric Chemistry and Physics*, 18, 65-79, 10.5194/acp-18-65-2018, 2018.
- Franchin, A., Ehrbart, S., Leppä, J., Nieminen, T., Gagne, S., Schobesberger, S., Wimmer, D., Duplissy, J., Riccobono, F., Dunne, E. M., Rondo, L., Downard, A., Bianchi, F., Kupc, A., Tsagkogeorgas, G., Lehtipalo, K., Manninen, H. E., Almeida, J., Amorim, A., Wagner, P. E., Hansel, A., Kirkby, J., Kurten, A., Donahue, N. M., Makhmutov, V., Mathot, S., Metzger, A., Petäjä, T., Schnitzhofer, R., Sipilä, M., Stozhkov, Y., Tome, A., Kerminen, V.-M., Carslaw, K., Curtius, J., Baltensperger, U., and Kulmala, M.: Experimental investigation of ion-ion recombination under atmospheric conditions, *Atmospheric Chemistry and Physics*, 15, 7203-7216, 2015.
- Gordon, H., Kirkby, J., Baltensperger, U., Bianchi, F., Breitenlechner, M., Curtius, J., Dias, A., Dommen, J., Donahue, N. M., Dunne, E. M., Duplissy, J., Ehrhart, S., Flagan, R. C., Frege, C., Fuchs, C., Hansel, A., Hoyle, C. R., Kulmala, M., Kürten, A., Lehtipalo, K., Makhmutov, V., Molteni, U., Rissanen, M. P., Stozhkov, Y., Tröstl, J., Tsakogeorgas, G., Wagner, R., Williamson, C., Wimmer, D., Winkler, P. M., Yan, C., and Carslaw, K. S.: Causes and importance of new particle formation in the present-day and preindustrial atmospheres. *Journal of Geophysical Research: Atmosphere*, 122, 8739-8760, 2017.
- Guo, S., Hu, M., Zamora, M. L., Peng, J., Shang, D., Zheng, J., Du, Z., Wu, Z., Shao, M., Zeng, L., Molina, M. J., and Zhang, R.: Elucidating severe urban haze formation in China, *Proceedings of the National Academy of Sciences of the United States of America*, 111, 17373-17378, 10.1073/pnas.1419604111, 2014.
- Hari, P., and Kulmala, M.: Station for measuring ecosystem-atmosphere relations, *Boreal Environment Research*, 10, 315-322, 2005.
- Heal, M., Kumar, P., and Harrison, R.: Particles, air quality, policy and health, *Chemical Society Reviews*, 41, 6606, 2012.
- Hirsikko, A., Laakso, L., Hörra, U., Aalto, P. P., Kerminen, V. M., and Kulmala, M.: Annual and size dependent variation of growth rates and ion concentrations in boreal forest, *Boreal Environ. Res.*, 10, Issue 5, 357-369, 2005.
- Hirsikko, A., Nieminen, T., Gagne, S., Lehtipalo, K., Manninen, H. E., Ehn, M., Horrak, U., Kerminen, V. M., Laakso, L., McMurry, P. H., Mirme, A., Mirme, S., Petaja, T., Tammet, H., Vakkari, V., Vana, M., and Kulmala, M.: Atmospheric ions and nucleation: a review of observations, *Atmospheric Chemistry and Physics*, 11, 767-798, 10.5194/acp-11-767-2011, 2011.

- Hoppel, W. A.: Ion-aerosol attachment coefficients, ion depletion, and the charge distribution on aerosols, *Journal of Geophysical Research*, 90, 5917-5923, 1985.
- Iida, K., Stolzenburg, M., McMurry, P., Dunn, M. J., Smith, J. N., Eisele, F., and Keady, P.: Contribution of ion-induced nucleation to new particle formation: Methodology and its application to atmospheric observations in Boulder, Colorado, *Journal of Geophysical Research: Atmospheres*, 111, n/a-n/a, 10.1029/2006jd007167, 2006.
- Jokinen, T., Sipilä, M., Junninen, H., Ehn, M., Lönn, G., Hakala, J., Petäjä, T., Mauldin Iii, R., Kulmala, M., and Worsnop, D.R.: Atmospheric sulphuric acid and neutral cluster measurements using CI-API-TOF, *Atmospheric Chemistry and Physics*, 12, 4117-4125, 2012.
- Junninen, H., Ehn, M., Petäjä, T., Luosujärvi, L., Kotiaho, T., Kostianinen, R., Rohner, U., Gonin, M., Fuhrer, K., and Kulmala, M.: A high-resolution mass spectrometer to measure atmospheric ion composition, *Atmospheric Measurement Techniques*, 3, 1039-1053, 2010.
- Kerminen, V.-M., Paramonov, M., Anttila, T., Riipinen, I., Fountoukis, C., Korhonen, H., Asmi, E., Laakso, L., Lihavainen, H., Swietlicki, E., Svenningsson, B., Asmi, A., Pandis, S. N., Kulmala, M., and Petäjä, T.: Cloud condensation nuclei production associated with atmospheric nucleation: a synthesis based on existing literature and new results, *Atmospheric Chemistry and Physics*, 12, 12037-12059, 2012, <https://doi.org/10.5194/acp-12-12037-2012>, 2012.
- Kirkby, J., Curtius, J., Almeida, J., Dunne, E., Duplissy, J., Ehrhart, S., Franchin, A., Gagné, S., Ickes, L., Kürten, A., Kupc, A., Metzger, A., Riccobono, F., Rondo, L., Schobesberger, S., Tsagkogeorgas, G., Wimmer, D., Amorim, A., Bianchi, F., Breitenlechner, M., David, A., Dommen, J., Downard, A., Ehn, M., Flagan, R. C., Haider, S., Hansel, A., Hauser, D., Jud, W., Junninen, H., Kreissl, F., Kvashin, A., Laaksonen, A., Lehtipalo, K., Lima, J., Lovejoy, E. R., Makhmutov, V., Mathot, S., Mikkilä, J., Minginette, P., Mogo, S., Nieminen, T., Onnela, A., Pereira, P., Petäjä, T., Schnitzhofer, R., Seinfeld, J. H., Sipilä, M., Stozhkov, Y., Stratmann, F., Tomé, A., Vanhanen, J., Viisanen, Y., Virtala, A., Wagner, P. E., Walther, H., Weingartner, E., Wex, H., Winkler, P. M., Carslaw, K. S., Worsnop, D. R., Baltensperger, U., and Kulmala, M.: Role of sulphuric acid, ammonia and galactic cosmic rays in atmospheric aerosol nucleation, *Nature*, 476, 429–433, <https://doi.org/10.1038/nature10343>, 2011.
- Kirkby, J., Duplissy, J., Sengupta, K., Frege, C., Gordon, H., Williamson, C., Heinritzi, M., Simon, M., Yan, C., Almeida, J., Tröstl, J., Nieminen, T., Ortega, I. K., Wagner, R., Adamov, A., Amorim, A., Bernhammer, A.-K., Bianchi, F., Breitenlechner, M., Brilke, S., Chen, X., Craven, J., Dias, A., Ehrhart, S., Flagan, R. C., Franchin, A., Fuchs, C., Guida, R., Hakala, J., Hoyle, C. R., Jokinen, T., Junninen, H., Kangasluoma, J., Kim, J., Krapf, M., Kürten, A., Laaksonen, A., Lehtipalo, K., Makhmutov, V., Mathot, S., Molteni, U., Onnela, A., Peräkylä, O., Piel, F., Petäjä, T., Praplan, A. P., Pringle, K., Rap, A., Richards, N. A. D., Riipinen, I., Rissanen, M. P., Rondo, L., Sarnela, N., Schobesberger, S., Scott, C. E., Seinfeld, J. H., Sipilä, M., Steiner, G., Stozhkov, Y., Stratmann, F., Tomé, A., Virtanen, A., Vogel, A. L., Wagner, A. C., Wagner, P. E., Weingartner, E., Wimmer, D., Winkler, P. M., Ye, P., Zhang, X., Hansel, A., Dommen, J., Donahue, N. M., Worsnop, D. R., Baltensperger, U., Kulmala, M., Carslaw, K. S., and Curtius, J.: Ion-induced nucleation of pure biogenic particles, *Nature*, 533, 521–526, <https://doi.org/10.1038/nature17953>, 2016.

- Kontkanen, J., Lehtinen, K. E. J., Nieminen, T., Manninen, H. E., Lehtipalo, K., Kerminen, V. M., and Kulmala, M.: Estimating the contribution of ion–ion recombination to sub-2 nm cluster concentrations from atmospheric measurements, *Atmospheric Chemistry and Physics*, 13, 11391–11401, 10.5194/acp-13-11391-2013, 2013.
- Kuang, C., Riipinen, I., Sihto, S. L., Kulmala, M., McCormick, A. V., and McMurry, P. H.: An improved criterion for new particle formation in diverse atmospheric environments, *Atmospheric Chemistry and Physics*, 10, 8469–8480, 10.5194/acp-10-8469-2010, 2010.
- Kulmala, M., Maso, M. D., Mäkelä, J. M., Pirjola, L., Väkevä, M., Aalto, P., Miikkulainen, P., Hämeri, K., and O'Dowd, C. D.: On the formation, growth and composition of nucleation mode particles, *Tellus B*, 53, 479–490, 2001.
- Kulmala, M., Vehkamäki, H., Petäjä, T., Dal Maso, M., Lauri, A., Kerminen, V.-M., Birmili, W., and McMurry, P. H.: Formation and growth rates of ultrafine atmospheric particles: a review of observations, *Journal of Aerosol Science*, 35, 143–176, 2004.
- Kulmala, M., Petaja, T., Nieminen, T., Sipila, M., Manninen, H. E., Lehtipalo, K., Dal Maso, M., Aalto, P. P., Junninen, H., Paasonen, P., Riipinen, I., Lehtinen, K. E., Laaksonen, A., and Kerminen, V. M.: Measurement of the nucleation of atmospheric aerosol particles, *Nature Protocol*, 7, 1651–1667, 10.1038/nprot.2012.091, 2012.
- Kulmala, M., Kontkanen, J., Junninen, H., Lehtipalo, K., Manninen, H. E., Nieminen, T., Petäjä, T., Sipilä, M., Schobesberger, S., Rantala, P., Franchin, A., Jokinen, T., Järvinen, E., Äijälä, M., Kangasluoma, J., Hakala, J., Aalto, P. P., Paasonen, P., Mikkilä, J., Vanhanen, J., Aalto, J., Hakola, H., Makkonen, U., Ruuskanen, T., Mauldin, R. L., Duplissy, J., Vehkamäki, H., Bäck, J., Kortelainen, A., Riipinen, I., Kurtén, T., Johnston, M. V., Smith, J. N., Ehn, M., Mentel, T. F., Lehtinen, K. E. J., Laaksonen, A., Kerminen, V.-M., and Worsnop, D. R.: Direct Observations of Atmospheric Aerosol Nucleation, *Science*, 339, 943–946, 10.1126/science.1227385, 2013.
- Kürten, A., Bianchi, F., Almeida, J., Kupiainen-Määttä, O., Dunne, E. M., Duplissy, J., Williamson, C., Barmet, P., Breitenlechner, M., Dommen, J., Donahue, N. M., Flagan, R. C., Franchin, A., Gordon, H., Hakala, J., Hansel, A., Heinritzi, M., Ickes, L., Jokinen, T., Kangasluoma, J., Kim, J., Kirkby, J., Kupc, A., Lehtipalo, K., Leiminger, M., Makhmutov, V., Onnela, A., Ortega, I. K., Petäjä, T., Praplan, A. P., Riccobono, F., Rissanen, M. P., Rondo, L., Schnitzhofer, R., Schobesberger, S., Smith, J. N., Steiner, G., Stozhkov, Y., Tomé, A., Tröstl, J., Tsagkogeorgas, G., Wagner, P. E., Wimmer, D., Ye, P., Baltensperger, U., Carslaw, K., Kulmala, M., and Curtius, J.: Experimental particle formation rates spanning tropospheric sulfuric acid and ammonia abundances, ion production rates, and temperatures, *Journal of Geophysical Research: Atmospheres*, 121, 12,377–312,400, 10.1002/2015jd023908, 2016.
- Lovejoy, E., Curtius, J., and Froyd, K.: Atmospheric ion-induced nucleation of sulfuric acid and water, *Journal of Geophysical Research: Atmospheres (1984–2012)*, 109, 2004.
- Makkonen, U., Virkkula, A., Hellen, H., Hemmila, M., Sund, J., Aijala, M., Ehn, M., Junninen, H., Keronen, P., Petaja, T., Worsnop, D. R., Kulmala, M., and Hakola, H.: Semi-continuous gas and inorganic aerosol measurements at a boreal forest site: seasonal and diurnal cycles of NH₃, HONO and HNO₃, *Boreal Environment Research*, 19, 311–328, 2014.

Manninen, H. E., Nieminen, T., Asmi, E., Gagne, S., Hakkinen, S., Lehtipalo, K., Aalto, P.,
 Vana, M., Mirme, A., Mirme, S., Horrak, U., Plass-Dulmer, C., Stange, G., Kiss, G., Hoffer,
 A., Toeroe, N., Moerman, M., Henzing, B., de Leeuw, G., Brinkenberg, M., Kouvarakis, G.,
 55 N., Bougiatioti, A., Mihalopoulos, N., O'Dowd, C., Ceburnis, D., Arneth, A., Svenningsson,
 B., Swietlicki, E., Tarozzi, L., Decesari, S., Facchini, M. C., Birmili, W., Sonntag, A.,
 Wiedensohler, A., Boulon, J., Sellegri, K., Laj, P., Gysel, M., Bukowiecki, N., Weingartner,
 E., Wehrle, G., Laaksonen, A., Hamed, A., Joutsensaari, J., Petaja, T., Kerminen, V. M., and
 Kulmala, M.: EUCAARI ion spectrometer measurements at 12 European sites - analysis of
 new particle formation events, *Atmospheric Chemistry and Physics*, 10, 7907-7927,
 10.5194/acp-10-7907-2010, 2010.

McMurry, P. H., Fink, M., Sakurai, H., Stolzenburg, M. R., Mauldin, R. L., Smith, J., Eisele,
 F., Moore, K., Sjostedt, S., and Tanner, D.: A criterion for new particle formation in the sulfur-
 rich Atlanta atmosphere, *Journal of Geophysical Research: Atmospheres*, 110, 2935-2948,
 2005.

Merikanto, J., Spracklen, D. V., Mann, G. W., Pickering, S. J., and Carslaw, K. S.: Impact of
 nucleation on global CCN, *Atmospheric Chemistry and Physics*, 9, 8601-8616, 10.5194/acp-9-
 8601-2009, 2009.

Mirme, S., and Mirme, A.: The mathematical principles and design of the NAIS-a spectrometer
 for the measurement of cluster ion and nanometer aerosol size distributions, *Atmospheric
 Measurement Techniques*, 6, 1061, 2013.

Riccobono, F., Schobesberger, S., Scott, C. E., Dommen, J., Ortega, I. K., Rondo, L., Almeida,
 J., Amorim, A., Bianchi, F., Breitenlechner, M., David, A., Downard, A., Dunne, E. M.,
 Duplissy, J., Ehrhart, S., Flagan, R. C., Franchin, A., Hansel, A., Junninen, H., Kajos, M.,
 Keskinen, H., Kupc, A., Kurten, A., Kvashin, A. N., Laaksonen, A., Lehtipalo, K.,
 Makhmutov, V., Mathot, S., Nieminen, T., Onnela, A., Petaja, T., Praplan, A. P., Santos, F. D.,
 Schallhart, S., Seinfeld, J. H., Sipila, M., Spracklen, D. V., Stozhkov, Y., Stratmann, F., Tome,
 A., Tsagkogeorgas, G., Vaattovaara, P., Viisanen, Y., Vrtala, A., Wagner, P. E., Weingartner,
 E., Wex, H., Wimmer, D., Carslaw, K. S., Curtius, J., Donahue, N. M., Kirkby, J., Kulmala,
 M., Worsnop, D. R., and Baltensperger, U.: Oxidation products of biogenic emissions
 contribute to nucleation of atmospheric particles, *Science*, 344, 717-721,
 10.1126/science.1243527, 2014.

Rose, C., Zha, Q., Dada, L., Yan, C., Lehtipalo, K., Junninen, H., Mazon, S. B., Jokinen, T.,
 Sarnela, N., Sipila, M., Petaja, T., Kerminen, V. M., Bianchi, F., and Kulmala, M.:
 Observations of biogenic ion-induced cluster formation in the atmosphere, *Science Advances*,
 4, eaar5218, 10.1126/sciadv.aar5218, 2018.

Schobesberger, S., Junninen, H., Bianchi, F., Lonn, G., Ehn, M., Lehtipalo, K., Dommen, J.,
 Ehrhart, S., Ortega, I. K., Franchin, A., Nieminen, T., Riccobono, F., Hutterli, M., Duplissy,
 J., Almeida, J., Amorim, A., Breitenlechner, M., Downard, A. J., Dunne, E. M., Flagan, R. C.,
 Kajos, M., Keskinen, H., Kirkby, J., Kupc, A., Kurten, A., Kurten, T., Laaksonen, A., Mathot,
 S., Onnela, A., Praplan, A. P., Rondo, L., Santos, F. D., Schallhart, S., Schnitzhofer, R., Sipila,
 M., Tome, A., Tsagkogeorgas, G., Vehkamäki, H., Wimmer, D., Baltensperger, U., Carslaw,
 K. S., Curtius, J., Hansel, A., Petaja, T., Kulmala, M., Donahue, N. M., and Worsnop, D. R.:
 Molecular understanding of atmospheric particle formation from sulfuric acid and large

oxidized organic molecules, *Proceedings of the National Academy of Sciences of the United States of America*, 110, 17223-17228, 10.1073/pnas.1306973110, 2013.

Schobesberger, S., Franchin, A., Bianchi, F., Rondo, L., Duplissy, J., Kurten, A., Ortega, I. K., Metzger, A., Schnitzhofer, R., Almeida, J., Amorim, A., Dommen, J., Dunne, E. M., Ehn, M., Gagne, S., Ickes, L., Junninen, H., Hansel, A., Kerminen, V. M., Kirkby, J., Kupc, A., Laaksonen, A., Lehtipalo, K., Mathot, S., Onnela, A., Petaja, T., Riccobono, F., Santos, F. D., Sipila, M., Tome, A., Tsagkogeorgas, G., Viisanen, Y., Wagner, P. E., Wimmer, D., Curtius, J., Donahue, N. M., Baltensperger, U., Kulmala, M., and Worsnop, D. R.: On the composition of ammonia-sulfuric-acid ion clusters during aerosol particle formation, *Atmospheric Chemistry and Physics*, 15, 55-78, 10.5194/acp-15-55-2015, 2015.

Stocker, T., Qin, D., Plattner, G., Tignor, M., Allen, S., Boschung, J., Nauels, A., Xia, Y., Bex, B., and Midgley, B.: IPCC, 2013: climate change 2013: the physical science basis. Contribution of working group I to the fifth assessment report of the intergovernmental panel on climate change, 2013.

Tammet, H., and Kulmala, M.: Simulation tool for atmospheric aerosol nucleation bursts, *Journal of Aerosol Science*, 36, 173-196, 2005.

Wagner, R., Yan, C., Lehtipalo, K., Duplissy, J., Nieminen, T., Kangasluoma, J., Ahonen, L. R., Dada, L., Kontkanen, J., Manninen, H. E., Dias, A., Amorim, A., Bauer, P. S., Bergen, A., Bernhammer, A. K., Bianchi, F., Brilke, S., Mazon, S. B., Chen, X. M., Draper, D. C., Fischer, L., Frege, C., Fuchs, C., Garmash, O., Gordon, H., Hakala, J., Heikkinen, L., Heinritzi, M., Hofbauer, V., Hoyle, C. R., Kirkby, J., Kurten, A., Kvashnin, A. N., Laurila, T., Lawler, M. J., Mai, H. J., Makhmutov, V., Mauldin, R. L., Molteni, U., Nichman, L., Nie, W., Ojdanic, A., Onnela, A., Piel, F., Quelever, L. L. J., Rissanen, M. P., Sarnela, N., Schallhart, S., Sengupta, K., Simon, M., Stolzenburg, D., Stozhkov, Y., Trostl, J., Viisanen, Y., Vogel, A. L., Wagner, A. C., Xiao, M., Ye, P., Baltensperger, U., Curtius, J., Donahue, N. M., Flagan, R. C., Gallagher, M., Hansel, A., Smith, J. N., Tome, A., Winkler, P. M., Worsnop, D., Ehn, M., Sipila, M., Kerminen, V. M., Petaja, T., and Kulmala, M.: The role of ions in new particle formation in the CLOUD chamber, *Atmospheric Chemistry and Physics*, 17, 15181-15197, 10.5194/acp-17-15181-2017, 2017.

Yan, C., Nie, W., Aijala, M., Rissanen, M. P., Canagaratna, M. R., Massoli, P., Junninen, H., Jokinen, T., Sarnela, N., Hame, S. A. K., Schobesberger, S., Canonaco, F., Yao, L., Prevot, A. S. H., Petaja, T., Kulmala, M., Sipila, M., Worsnop, D. R., and Ehn, M.: Source characterization of highly oxidized multifunctional compounds in a boreal forest environment using positive matrix factorization, *Atmospheric Chemistry and Physics*, 16, 12715-12731, 10.5194/acp-16-12715-2016, 2016.